

2*p* absorption spectra of the 3*d* elements

J. Fink, Th. Müller-Heinzerling, and B. Scheerer

*Kernforschungszentrum Karlsruhe, Institut für Nukleare Festkörperphysik, Postfach 3640,
D-7500 Karlsruhe, Federal Republic of Germany*

W. Speier and F. U. Hillebrecht

*Institut für Festkörperforschung, Kernforschungsanlage Jülich, Postfach 1913,
D-5170 Jülich, Federal Republic of Germany*

J. C. Fuggle

Fysische Chemie, Faculteit der Wetenschappen, Katholieke Universiteit Nijmegen, 6524 ED Nijmegen, The Netherlands

J. Zaanen and G. A. Sawatzky

*The Physical Chemistry Department of the Material Science Center, Nijenborgh 16, 9747 AG Groningen, The Netherlands
(Received 29 April 1985)*

The near-edge structure of the 2*p* absorption edges of the complete series of the 3*d* transition metals has been investigated by high-resolution electron-energy-loss spectroscopy. Structures in the spectra were observed that could not be resolved in previous studies. The data are compared with single-particle calculations of the 2*p*→3*d* transition probability as well as with bremsstrahlung isochromat spectra. The comparison shows that the absorption spectra cannot be described by the density of unoccupied *d* states even when single-particle matrix-element effects are taken into account. Especially at the beginning of the 3*d* series, the interaction with the core hole is an important parameter.

I. INTRODUCTION

In core-level absorption spectroscopy, transitions from a narrow core level to the unoccupied conduction states are investigated. Thus to a first approximation the structure in the region of the core edges can be associated with the unoccupied density of states (DOS). However, there has been much discussion over many years on the possible effect of the core-hole potential on absorption spectra¹⁻³ and on the role of matrix-element effects.⁴ In the free-electron-like metals the most generally recognized effects are the enhancement or the reduction at the threshold due to many-body effects.^{5,6} At higher energies above the edge it is generally recognized for the simple metals that the core-hole potential has relatively little effect on the observed spectra. At the other extreme, in the rare earths where very localized wave functions contribute to the final states, it is quite clear that in the atomiclike spectra observed for the *d*→4*f* transitions the core-hole-4*f* interaction is very large and lowers the energy of these transitions by ~10–20 eV with respect to the *d*-conduction-band edge.^{7,8} In addition, it is recognized from atomic calculations that the statistical spin-orbit weights for core-level edges will only arise if the spin-orbit splitting is much larger than the electron-hole exchange interaction (i.e., if $\Delta_{SO}^{2p} \gg \langle 2p V | 1/r_{12} | V 2p \rangle$ where *V* is the valence state occupied in the transition 2*p*→*V*). In general this coupling transfers weight from the lower to the higher of the edges in a spin-orbit doublet.⁹⁻¹² Such nonstatistical weights have been observed for many cases where the atomic calculations are valid, such as the 3*d*→4*f* transi-

tions of La (Refs. 13 and 14) or the 5*d*→5*f* absorption of Th and U (Refs. 12, 15, and 16).

We will argue that all the effects described above play a role in the 2*p* absorption spectra of the 3*d* transition metals (TM's) which are not quantitatively understood at present. This explains why every improvement in experimental resolution has brought new puzzles to light in these spectra. Early experiments¹⁷ were explained in terms of the unoccupied DOS but latter experiments indicated that the complex structures of the *L*_{2,3} edges of TiC, TiN, VC, and VN were different for the *L*₂ and *L*₃ edges and could not be explained in terms of the local 3*d* DOS in these compounds.¹⁸ Further, the experimental ratio of the *L*₃ to the *L*₂ edge intensity is not 2:1,¹⁸⁻²⁰ but frequently much less for the early TM's.

In this paper we present systematic, high-resolution absorption spectra of the *L*_{2,3} near-edge structure of all the 3*d* TM's and show how the effects described in the companion paper²¹ develop across the 3*d* series. Due to the high resolution, we find new structures not resolved in lower-resolution studies. We compare the absorption spectra with bremsstrahlung isochromat spectra (BIS) and with single-particle calculations of the 2*p*→3*d* transition probability in order to quantify the discrepancies which arise when a total DOS and single-particle matrix elements are used to analyze the absorption spectra of these metals. In the companion paper²¹ we show that for the early transition metals many of these puzzles can be explained by a complex interplay of atomic and DOS effects.

The absorption spectra presented here were recorded by

electron energy-loss spectroscopy (EELS). The advantage of this method over x-ray absorption spectroscopy is that measurements with high and constant resolution over an energy range of 0 to ~ 2000 eV are possible. The cross section for inelastic high-energy electron scattering into small angles is given in the Born approximation by²²

$$\frac{d^2\sigma(E, q)}{dE dq} = \frac{8\pi e^4}{\hbar^2 v^2} \frac{1}{q^3} |\langle f | \exp(i\mathbf{q}\cdot\mathbf{r}) | i \rangle|^2 \\ \rightarrow \frac{8\pi e^4}{\hbar\omega^2} \frac{1}{q} |\langle f | \hat{\mathbf{e}}_q \cdot \mathbf{r} | i \rangle|^2, \text{ for } q \ll r_c^{-1},$$

where \mathbf{q} is the momentum transfer, E is the energy loss, v is the incident electron velocity, and $\hat{\mathbf{e}}_q$ is a unit vector in the direction of \mathbf{q} . For small momentum transfer compared to the radius r_c of the core level, we get for independent electrons (Hartree approximation) the same matrix elements as for x-ray absorption spectroscopy, i.e., only dipole transitions are allowed, and thus quadrupole transitions can be neglected. For the case of the $2p$ absorption in $3d$ TM elements, this means, that due to the dipole selection rules ($\Delta l = \pm 1$) only final states with s or d symmetry are reached. As $|\langle 2p | r | 4s \rangle|^2 \ll |\langle 2p | r | 3d \rangle|^2$ and as the density of states of the $4s$ band is considerably lower than that of the $3d$ band, the near-edge structure of the $L_{2,3}$ edges is more closely related to empty $3d$ states.

II. EXPERIMENTAL

The metallic films having a thickness of 600 to 1000 Å were prepared by electron-beam evaporation or by evaporation from a molybdenum boat in an ultrahigh-vacuum (UHV) system having a base pressure of better than 1×10^{-9} Torr. The film thickness was monitored using a quartz crystal close to the substrate which was for the heavier TM's a 100-Å-thick amorphous carbon layer on a standard electron-microscopy grid. In those cases where a reaction of the $3d$ TM with the carbon substrate was suspected or observed (Ca, Sc, Ti, V, Cr, Mn), a thin film (~ 200 Å) of Pioloform F (Wacker Chemie, Munich) was used as a substrate. The metal films obtained in this way were transferred under ultrahigh-vacuum conditions to the ELS spectrometer having a vacuum of about 5×10^{-10} Torr. The samples were characterized by taking diffraction patterns in the EELS spectrometer with a resolution of 0.04 \AA^{-1} . With this method we can detect less than 5% of impurity phases such as oxides. None of the films used here contained detectable impurities.

The EELS spectra were taken in transmission using an electron beam with an energy of 170 keV. The major elements of the spectrometer are an electron gun, a monochromator, zoom lenses, an accelerator, a chamber containing the sample and deflection plates, a decelerator, zoom lenses, an analyzer, and a detector. The energy resolution can be varied between 0.08 and 0.6 eV by changing the pass energy of the monochromator and the analyzer. The momentum resolution can be varied between 0.04 and 0.2 \AA^{-1} by changing the voltages on the zoom lenses. As the sample was at ground potential, it was possible to attach the sample preparation chamber to

the chamber for the sample in the EELS spectrometer. Details of the spectrometer are described elsewhere.²³ The BIS spectra were recorded at a photon energy of 1486 eV and a resolution ~ 0.65 eV in an UHV system. The samples were treated with either Ar-ion etching or scraping, and surface composition was checked with x-ray-induced photoemission spectroscopy (XPS) and Auger electron spectroscopy.²⁴

III. RESULTS

In Fig. 1 we illustrate the $L_{2,3}$ absorption spectra for all the $3d$ TM's after background subtraction. The spectra from Ca to V were taken with an energy and momentum resolution of 0.2 eV and 0.1 \AA^{-1} , respectively. The other metals were measured with an energy and momentum resolution of 0.6 eV and 0.2 \AA^{-1} , respectively, to increase the counting rate. The spectra were aligned according to the binding energies of the $2p_{3/2}$ level as derived from the EELS spectra. In the cases of Ca, Sc, Ti, and V the binding energy can be extracted very accurately as in these spectra sharp edges with a width of 0.3 eV for Ca and 0.5 eV for Sc, Ti, and V are observed. For the other metals, the edges are less pronounced and thus the binding energy was derived by extrapolating the L_3 edge to the background line. The binding energies of the $2p_{3/2}$ level are listed in Table I and compared with those derived from XPS.²⁵ In addition the apparent EELS spin-orbit splitting, derived from the separation of peaks between L_3 and L_2 lines is compared in Table I with spin-orbit splittings given in the literature.²⁵ Differences of up to 0.8 eV, espe-

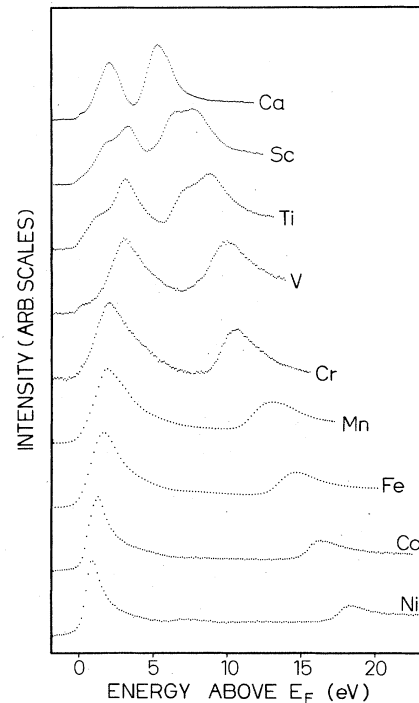


FIG. 1. $L_{2,3}$ edges of the $3d$ metals Ca–Ni.

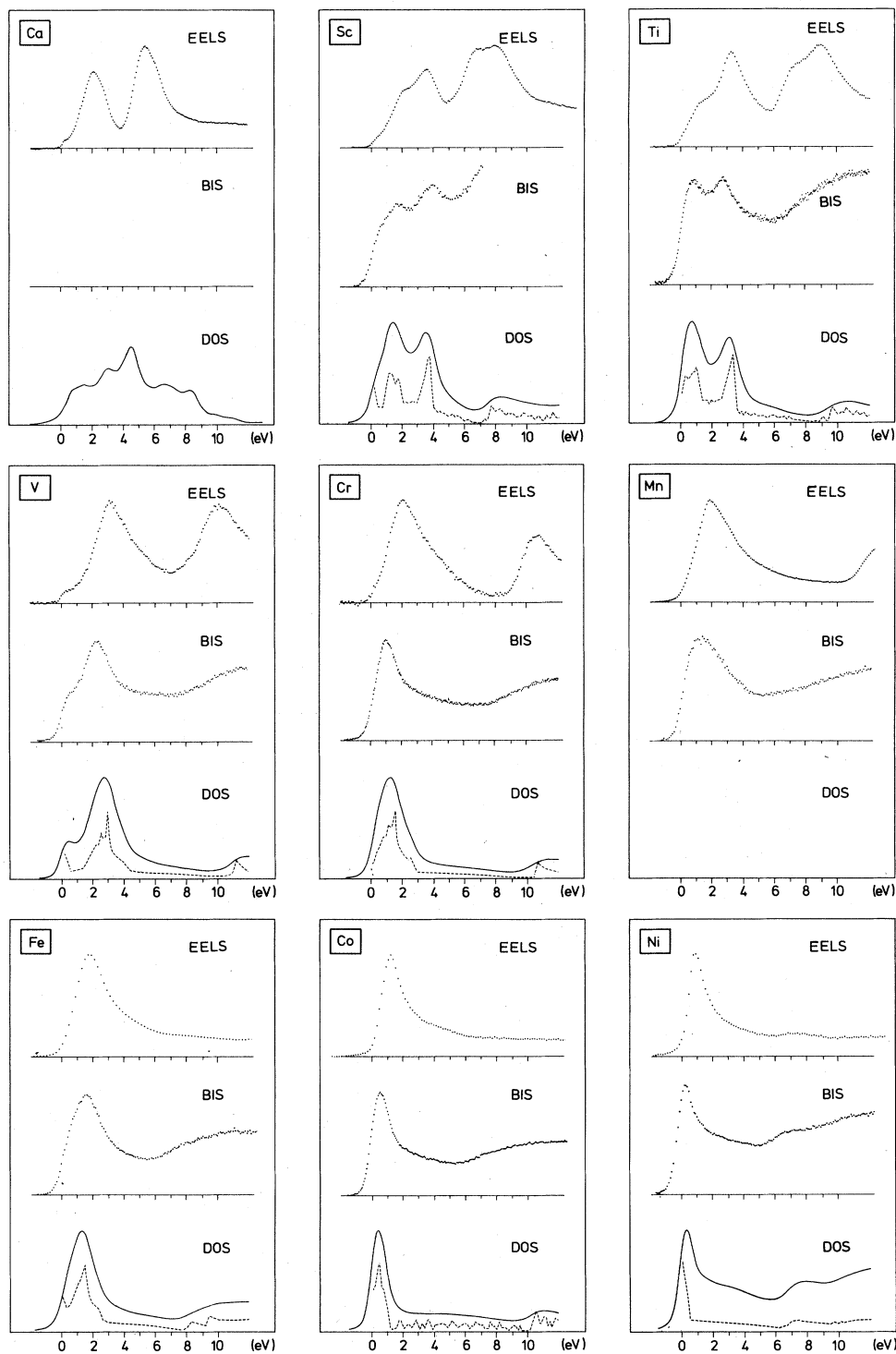


FIG. 2. Comparison of the EELS $L_{2,3}$ edges with broadened DOS curves and with BIS spectra. For Ca, the EELS spectrum is compared with a calculation of a single-particle $L_{2,3}$ edge using a calculated DOS and neglecting matrix-element effects. The ordinates are given in arbitrary scales. The abscissa gives the energy above the L_3 threshold for EELS and the energy above the Fermi energy for BIS spectra and DOS.

cially for the light 3d metals are realized. The agreement between EELS and XPS binding energies is excellent for the first half of the 3d series. For the heavier elements the deviations are marginally larger but are not experi-

mentally significant.

The spectra in Fig. 1 reveal very clearly that there are deviations from the statistical intensity ratio of 2:1 for the $2p_{3/2}$ and $2p_{1/2}$ lines. In Ni the ratio is near 2:1 and the

TABLE I. $3d$ -metal XPS and EELS binding energies (see footnote a) E_B for the L_3 shell, spin-orbit splitting (see footnote a) Δ_{SO} and differences δ between XPS and EELS values. All values are given in eV.

| | XPS ^a | | EELS ^a | | δ_{E_B} | δ_{SO} |
|----|------------------|---------------|-------------------|---------------|----------------|---------------|
| | E_B | Δ_{SO} | E_B | Δ_{SO} | | |
| Ca | 346.0 | 3.7 | 346.1 | 3.2 | -0.1 | 0.5 |
| Sc | | 4.9 | 398.4 | 4.2 | | 0.7 |
| Ti | 453.9 | 6.2 | 453.8 | 5.7 | 0.1 | 0.5 |
| V | 512.1 | 7.7 | 512.0 | 6.9 | 0.1 | 0.8 |
| Cr | 574.3 | 9.3 | 574.3 | 8.5 | 0.0 | 0.8 |
| Mn | 638.8 | 11.1 | 638.5 | 11.0 | 0.3 | 0.1 |
| Fe | 706.7 | 13.2 | 706.6 | 12.9 | 0.1 | 0.3 |
| Co | 778.3 | 14.6 | 777.6 | 14.9 | 0.7 | -0.3 |
| Ni | 852.8 | 17.3 | 851.9 | 17.2 | 0.9 | 0.1 |

^aFrom Ref. 25 (XPS) and this work (EELS).

integrated $2p_{3/2}$ edge intensity may actually be more than twice that of the $2p_{1/2}$. However, this changes in the early $3d$ TM's and in Ca and Sc the L_2 edge is clearly more intense than the L_3 edge. Because we have measured the complete $3d$ series, we see that there is a continuous change on going from Ni to Ca, in agreement with the results of Leapman and Grunes.^{19,20}

The spectra shown in Fig. 1 contain two groups of peaks near the L_2 and L_3 thresholds. There is structure in the early TM spectra which has not been observed previously. This is shown more clearly in Fig. 2. There we present EELS and BIS spectra for the metals Ca to Ni and compare them with theoretical calculations of the DOS.²⁴ The theoretical curves are broadened by a Lorentzian in order to include experimental resolution and lifetime effects. We note, that in both BIS and EELS curves there is structure in the d bands above E_F . In the BIS spectra, the peak positions are in reasonable agreement with DOS calculations and only differences in the relative intensities with respect to the DOS are observed. When we compare the EELS peaks we find that not only are the peak positions different from those found in BIS and DOS curves, but the separations from the thresholds are up to ~ 1 eV different in L_2 and L_3 spectra of the early transition metals (see Table II). For the L_2 edge, XPS values are taken for the threshold. This is reasonable

because of the excellent agreement of the XPS- and EELS-derived binding energies for the $2p_{3/2}$ electrons. The different peak positions relative to the L_2 and L_3 thresholds lead then to the apparent difference of the spin-orbit splitting observed in EELS and in photoemission spectroscopy.

IV. DISCUSSION

We first discuss those points relevant to our main objective of preparing a foundation for discussion of many-body interactions by quantifying the experimental data and any possible effects due to single-particle matrix elements. The salient experimental observations which must be explained are the divergence from the expected 2:1 statistical weights for the ratio of the L_3 to L_2 peak intensities and the differences in shape between L_3 and L_2 spectral regions and between the EELS spectra and the DOS.

Four effects are at present cataloged in the literature, which must be considered in the light of experimental observations. These are the energy dependence of the single-particle optical transition matrix elements, atomic multiplet effects within the ground state wave function, the Coulomb and exchange interactions between the core hole and the d electrons which we split into the monopole-like attractive potential and the higher-multipole Coulomb and exchange interactions.

The origin of the single-particle matrix-element effects arises from the fact that in general the radial part of the atomic d wave function is dependent on the k vector and therefore is dependent on the energy. In the tight-binding approximation, the radial part of the atomic wave function is assumed to be independent of energy and therefore the transition matrix elements are constant within the d band. However, for the early transition metals the atomic d wave functions have a considerable overlap with those centered on nearest neighbors. In this case orthogonalization will cause the d amplitude in the core region to decrease for the bondinglike states and increase for the antibondinglike states. Since the bottom of the d band is bondinglike and the top is antibondinglike one could expect the transition matrix elements to increase with energy. However, a comparison with calculations including matrix-element effects shows that their influence is much

TABLE II. Separations of the major peaks from E_F in BIS and DOS spectra or from the $L_{2,3}$ edges in EELS spectra (all values in eV).

| | Experimental | EELS | Experimental | Theoretical |
|----|----------------|----------|--------------|------------------|
| | L_3 | L_2 | BIS | DOS |
| Ca | 2.1 | 1.7 | | 1, 3, 4.2 |
| Sc | 2.1, 3.5 | 1.8, 3.0 | 1.8, 3.8 | 1.4, 3.5 |
| Ti | 1.3, 3.3 | 1.2, 2.7 | 1.0, 2.8 | 0.8, 3.1 |
| V | ~ 0 , 3.1 | 2.3 | 2.3 | ~ 0.5 , 2.5 |
| Cr | 2.2 | 1.1 | 1.0 | 1.2 |
| Mn | 2.0 | 1.3 | 1.4 | |
| Fe | 1.7 | 1.1 | 1.6 | 1.6 |
| Co | 1.2 | 0.8 | 0.5 | 0.5 |
| Ni | 0.9 | 0.1 | 0.3 | 0.3 |

too small to explain the experimental spectra. For example, in Fig. 3 we see, that single-particle matrix-element corrections for Ti only renormalize the intensity at E_f by 30% with respect to the top of the band.⁴

The second major effect we consider is that of the atomiclike multiplets caused by electron correlation effects in the ground-state wave functions. These effects have been observed in the $2p \rightarrow 3d$ transitions of TM's in environments where the $3d$ electrons are highly correlated giving rise to atomiclike ground states.²⁶ However, certainly for the early TM's, the success of one-electron band theory in describing the valence-band structure²⁴ rules out large effects due to electron correlation in the d band.

The third major effect to be considered are core-hole-potential effects. Here we note that the agreement between BIS and DOS is often better than between EELS and DOS, e.g., for Cr the BIS and DOS peaks are at 1.0 and 1.2 eV; the $L_{2,3}$ peaks are at ~ 1.1 and 2.2 eV, respectively. As BIS differs from EELS in exhibiting no core-hole effects, this suggests that core-hole potential effects may be important in the $2p$ EELS spectra. However, in other spectroscopies^{27,28} and in calculations of impurities in a TM matrix²⁸ one universally finds a shift of local DOS features on a $Z+1$ element to lower energies with respect to those of the matrix. Also, nothing in the literature suggests why the influence of the core hole (potential) should be different for the L_2 and L_3 holes. In contrast, the features we find in the spectra are dissimilar in the L_2 and L_3 regions and the peaks are often found at higher energies: for instance in Cr the L_3 feature is ~ 1 eV higher than that found in the DOS. In fact, we do not dismiss the effect of the core-hole potential for the TM elements but we show in the companion paper²¹ that its effects interact with other effects present and the results are too subtle to be taken into account by simply calculating the local density of states around a $Z+1$ impurity.

The fourth effect we consider is the exchange interaction $G = \langle 2p\ 3d | 1/r_{12} | 3d\ 2p \rangle$. This atomiclike effect can lead to significant transfer of weight from the L_2 to the L_3 edges if G is comparable to the spin-orbit couplings Δ_{SO} .⁹⁻¹² The observation in the early TM's of a large decrease in the L_3 to L_2 weight ratio with respect to the statistical 2:1 ratio is compatible with the smaller

values of Δ_{SO} in these elements. However, the atomiclike effect of G cannot explain the differences between L_2 and L_3 edge shapes or the other experimental observations and so it should not be treated in isolation for a solid TM.

Finally we discuss the results on the lifetime of the $2p_{3/2}$ core level. The observed width of the steplike L_3 edge in Ca is 0.3 eV and in Sc, Ti, and V it is 0.5 eV. This corresponds to a folding of a step function with a Lorentzian with a full width at half maximum of about 70% of the observed width. Taking into account the experimental resolution of 0.2 eV we obtain a lifetime broadening for the $2p_{3/2}$ level for Ca, $\Gamma \leq 0.1$ eV and for Sc, Ti, and V $\Gamma \leq 0.2$ eV. These values are close to the results of semiempirical calculations of Krause and Oliver.²⁹ The EELS-derived $2p$ level width of V is also close to the value $\Gamma = 0.18$ eV extracted from Auger electron spectroscopy.³⁰ However, the EELS values for Ti and V are much smaller than the level width found in XPS by Fuggle and Alvarado³¹ (Ti, $\Gamma = 0.75$ eV; V, $\Gamma = 0.45$ eV). This is a very significant observation. In a study of core-level lifetime broadening for the whole periodic table of the elements Fuggle and Alvarado³¹ found an increase in observed XPS linewidth for the $2p$ levels in the middle of the TM series that was not predicted by the theory. They could not prove adequately whether or not this was related to lifetime broadening. The observation of narrower features in the L_3 EELS spectra shows that it was not lifetime related at all. In fact the observation of these narrow features in EELS highlights two difficulties in the interpretation of XPS line shapes. The first is that there are complications due to dynamics of screening of a core hole by a d electron.³²⁻³⁴ This is a much smaller problem in the $2p$ absorption spectra in which the primary excitation is $2p \rightarrow 3d$ and to a first approximation no screening is necessary. The second point is that in XPS spectra any atomiclike multiplet effects are difficult to see because selection rules do not forbid any of the final-state lines in the "well-screened" final states and no structure is usually discernable.³⁵ This is because the screening electron taken from the band can have any values of S and J necessary to satisfy the selection rules. By contrast, in absorption spectroscopy, the dipole selection rules select out a small part of the multiplet states and multiplet structure can be recognized as such.²⁶

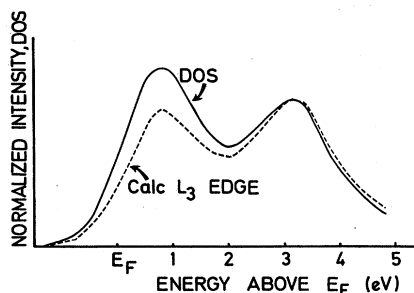


FIG. 3. A comparison of a broadened DOS of Ti metal with the calculated single-particle transition probability for the Ti L_3 edge (DOS weighted by single-particle matrix elements). The latter curve has been normalized to the first at the high-energy peak.

V. CONCLUSION

High-resolution spectra of all 3d TM's have been recorded by EELS. For the light 3d TM's, information on the lifetime of the $2p$ core levels is obtained. A comparison with values derived by XPS reveals that screening of a core hole is more complicated in XPS than in absorption spectroscopy and/or that broadening of core-level spectra due to multiplet splitting is stronger in XPS than in XAS or EELS. We have shown that the detailed shape of the $L_{2,3}$ edges in the 3d TM can be explained neither on the basis of a purely atomiclike picture as in the $3d \rightarrow 4f$ transitions of the rare-earth metals, nor on the basis of the structure in the DOS above E_f with small modifications due to single-particle matrix elements. The

major anomalies that must be explained are the following.

(1) The major differences in the early TM's between the L_3 and L_2 weights observed in XAS and EELS and the statistical spin-orbit splitting ratio of 2:1.

(2) The differences between the shape of the $L_{2,3}$ edges on the one hand and the BIS or DOS shapes on the other.

(3) The differences between the L_3 and L_2 edge shapes.

In the following paper we will show how these effects can be qualitatively explained by a combination of the atomlike $2p$ - $3d$ exchange interaction, the potential of

the core hole created, and the local DOS around a TM atom in the solid.

ACKNOWLEDGMENTS

We thank J.E. Müller and R. Zeller for extensive discussions and provision of unpublished results. We are also grateful to J. Keppels for technical assistance and M. Campagna and W. Schmatz for their encouragement of this line of work.

-
- ¹L. G. Paratt, *Rev. Mod. Phys.* **31**, 616 (1959).
²F. C. Brown, *Solid State Phys.* **29**, 1 (1974).
³C.-O. Almbladh and L. Hedin, in *Handbook on Synchrotron Radiation*, edited by E. E. Koch (North-Holland, Amsterdam, 1983), Vol. 1B, p. 607.
⁴J. E. Müller, O. Jepsen, and J. W. Wilkins, *Solid State Commun.* **42**, 365 (1982).
⁵G. D. Mahan, *Phys. Rev.* **163**, 612 (1967).
⁶P. H. Citrin, G. K. Wertheim, and M. Schlüter, *Phys. Rev. B* **20**, 3067 (1979).
⁷J. C. Fuggle, F. U. Hillebrecht, J.-M. Esteva, R. C. Karnatak, O. Gunnarsson, and K. Schönhammer, *Phys. Rev. B* **27**, 4637 (1983).
⁸O. Gunnarsson and K. Schönhammer, *Phys. Rev. B* **28**, 4315 (1983).
⁹M. W. D. Mansfield, *Proc. R. Soc. London, Ser. A* **348**, 143 (1976).
¹⁰J. Barth, F. Gerken, and C. Kunz, *Phys. Rev. B* **28**, 3608 (1983).
¹¹H. Nakamura, K. Ichikawa, T. Watanabe, and K. Tsutsumi, *Phys. Soc. Jpn.* **52**, 4014 (1983).
¹²G. Wedin, *Phys. Rev. Lett.* **53**, 727 (1984), and references therein.
¹³R. C. Karnatak, J.-M. Esteva, and J. P. Connerate, *J. Phys. B* **14**, 4727 (1981).
¹⁴P. Motais, E. Belin, and C. Bonnelle, *J. Phys. F* **11**, L169 (1981).
¹⁵M. Cukier, P. Dhez, B. Gauthé, P. Jaeglé, Cl. Wehenkel, and F. Combet Farnoux, *J. Phys.* **39**, L315 (1978).
¹⁶J. P. Connerade, M. Pantetouris, M. A. Baig, M. A. P. Martin, and M. Cukier, *J. Phys. B* **13**, L354 (1980).
¹⁷Ch. Bonnelle, *Ann. Phys. (Paris)* **1**, 439 (1966).
¹⁸J. Pflüger and J. Fink (unpublished).
¹⁹R. D. Leapman and L. A. Grunes, *Phys. Rev. Lett.* **45**, 398 (1980).
²⁰R. D. Leapman, L. A. Grunes, and P. L. Fejes, *Phys. Rev.* **26**, 614 (1982).
²¹J. Zaanen, G. A. Sawatzky, J. Fink, W. Speier, and J. C. Fuggle, following paper, *Phys. Rev. B* **32**, 4905 (1985).
²²H. A. Bethe, *Ann. Phys. (Leipzig)* **5**, 325 (1930).
²³J. Fink, Th. Müller-Heinzerling, J. Pflüger, A. vom Felde, and B. Scheerer, in *Proceedings of the International Conference on X-ray and Inner-Shell Processes in Atoms, Molecules and Solids*, edited by A. Meisel and J. Finster (Karl-Marx-Universität, Leipzig, GDR, 1984), p. 425.
²⁴W. Speier, J. C. Fuggle, R. Zeller, B. Ackermann, K. Szot, F. U. Hillebrecht, and M. Campagna, *Phys. Rev. B* **30**, 6921 (1984).
²⁵J. C. Fuggle and N. Martensson, *J. Electron Spectrosc. Relat. Phenom.* **21**, 275 (1980).
²⁶B. T. Thole, R. D. Cowan, G. A. Sawatzky, J. Fink, and J. C. Fuggle, *Phys. Rev. B* **31**, 6856 (1985).
²⁷R. Lässer and J. C. Fuggle, *Phys. Rev. B* **22**, 2637 (1980).
²⁸J. Deutz, P. H. Dederichs, and R. Zeller, *J. Phys. F* **11**, 1787 (1981), and references therein.
²⁹M. O. Krause and J. H. Oliver, *J. Phys. Chem. Ref. Data* **8**, 328 (1979).
³⁰R. Nyholm, M. Martensson, A. Lebugle, and U. Axelsson, *J. Phys. F* **11**, 1727 (1981).
³¹J. C. Fuggle and S. F. Alvarado, *Phys. Rev. A* **22**, 1615 (1980).
³²S. Doniac and M. Šunjić, *J. Phys. C* **3**, 285 (1970).
³³J. C. Fuggle, M. Campagna, Z. Zolnieriek, R. Lässer, and A. Platau, *Phys. Rev. Lett.* **45**, 1597 (1980).
³⁴O. Gunnarsson and K. Schönhammer, *Phys. Rev. B* **26**, 2765 (1982).
³⁵J.-M. Esteva, R. C. Karnatak, J. C. Fuggle, and G. A. Sawatzky, *Phys. Rev. Lett.* **50**, 910 (1983).